Theoretical and experimental investigations of the controlled motion of the Roller Racer

1st Kirill S. Yefremov
Kalashnikov Izhevsk State Technical University
Izhevsk, Russia
efremofk@yandex.ru

2nd Tatiana B. Ivanova
Udmurt State University
Izhevsk, Russia
tbesp@rcd.ru

3rd Alexander A. Kilin
Udmurt State University
Izhevsk, Russia
aka@rcd.ru

4th Yury L. Karavaev
Kalashnikov Izhevsk State Technical University
Izhevsk, Russia
Chuvash State University
Cheboksary, Russia
Center for Technologies in Robotics and Mechatronics Components
Innopolis University
Innopolis, Russia
karavaev_yury@istu.ru

***Abstract*—In this paper we address the problem of the motion of the Roller Racer. We assume that the angle $\varphi(t)$ between the platforms is a prescribed function of time and that the no-slip condition (nonholonomic constraint) and viscous friction force act at the points of contact of the wheels. In this case, all trajectories of the reduced system asymptotically tend to a periodic solution. In this paper it is shown analytically and experimentally that the chosen control defines periodic trajectories of the attachment point of the platforms on an average along a straight line. We determine the conditions for optimal control when the system moves along a straight line depending on the mass and geometric characteristics of the system and control parameters.**

***Index Terms*—Roller Racer, nonholonomic constraint, viscous friction, control, periodic solution**

I. Introduction

The Roller Racer is a system consisting of two platforms (connected to each other by means of a cylindrical joint). The platforms can rotate in a horizontal plane relative to each other. Each platform has a rigidly attached wheel pair consisting of two wheels lying on the same axis. The propulsion of the Roller Racer is possible due to periodic oscillations of the platform relative to each other.

The equations of motion of the Roller Racer involve a large number of parameters. Therefore, as a rule, this system is considered under some restrictions on the position of the center of mass of each platform [1]–[3]. In this paper we assume that the center of mass of each platform is on its symmetry axis and two principal axes of inertia lie in the plane parallel to the plane of rolling of the system. In the most general form the dynamics of the inertial motion of the Roller Racer is examined in [4].

The authors of [5] address the problem of the motion of the Roller Racer in which the angle $\varphi(t)$ between the platforms is a prescribed periodic function of time. Equations of motion are obtained for a fairly general mass distribution of the platforms. It is proved that, in the general case, when the viscous friction forces act on the system at the point of contact of the wheels with the plane, there is no constant acceleration of the Roller Racer and all trajectories of the reduced system asymptotically tend to a periodic solution.

We also mention references [6]–[8], in which the problem of the motion of a wheeled vehicle with two wheel pairs are considered. In these papers a complete classification of possible types of motion is presented and their dynamics are analyzed for two particular cases of wheeled vehicles (a symmetric vehicle with one fixed axle and a symmetric vehicle with unfixed axles). Similar mechanisms are investigated also in [9]–[11].

In this paper we investigate theoretically and experimentally the motion of the Roller Racer depending on the mass and geometric parameters of the system and for different control functions $\varphi(t)$. We define numerically optimal parameters at which the periodic motion corresponds to the largest average value of the velocity of the periodic solution.

It is shown experimentally that the nonholonomic motion model that has been chosen to describe the system and takes viscous friction into account provides an adequate description of the observed motion. The trajectory of the full-scale specimen of the Roller Racer qualitatively coincides with the theoretically calculated trajectory and corresponds to the found conditions for optimal motion.

II. Equations of motion

Consider the problem of the motion of the Roller Racer on a plane relative to an inertial coordinate system Oxy. The

The work of A. A. Kilin and T. B. Ivanova was carried out within the framework of the state assignment of the Ministry of Education and Science of Russia (FEWS-2020-0009) and was supported by the RFBR Grant 18-08-00999-a. The work of Yefremov K. S. and Karavaev Y. L. was carried out within the framework of the state assignment of the Ministry of Education and Science of Russia (FZZN-2020-0011). The experimental investigations were carried out using the equipment of the Common Use Center of the Udmurt State University.

978-1-7281-8763-1/20/$31.00 ©2020 IEEE

plane Oxy coincides with the plane of motion (Fig. 1). Table I presents the symbols used in this paper.

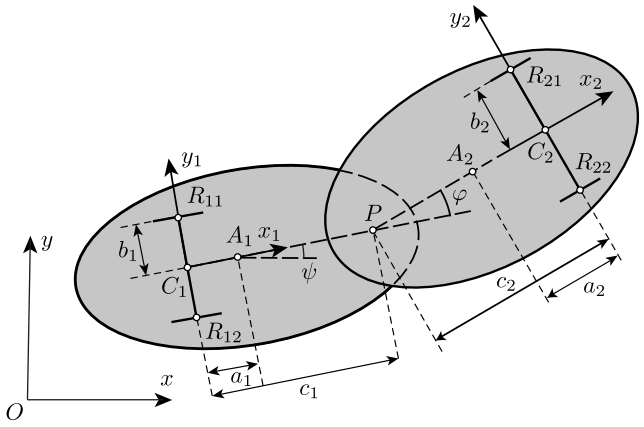

Fig. 1. The Roller Racer on a plane

TABLE I
SYMBOLS

φ	the angle between the axes C_1x_1 and C_2x_2 (the orientation of the platforms relative to each other)
ψ	the angle between the axes Ox and C_1x_1 (the orientation of the first platform relative to the fixed coordinate system)
h	the radius of the wheels on the first and second platforms
$\boldsymbol{r} = (x, y, h)$	the radius vector of the point of attachment of the platforms, P, in the fixed coordinate system Oxy
c_1, c_2	distances from the center of the first and second wheel pairs to point P
a_1, a_2	distances from point C_1 to the center of mass of the first platform and from point C_2 to the center of mass of the second platform
m_1, m_2	the masses of the first and second platforms
I_{10}, I_{20}	the moments of inertia of the first and second platforms relative to their centers of mass (points A_1 and A_2)
κ_1, κ_2	coefficients of viscous friction
b_1, b_2	distances from the point of contact of the wheels to the center of mass of the corresponding wheel pair

We assume that there is no slipping at the points of contact of the wheels with the plane. The corresponding constraint equations can be written in the form [5]

$$\begin{gathered} -\dot{x}\sin\psi + \dot{y}\cos\psi + c_1\dot{\psi} = 0, \\ -\dot{x}\sin(\varphi(t)+\psi) + \dot{y}\cos(\varphi(t)+\psi) - c_2(\dot{\varphi}(t)+\dot{\psi}) = 0. \end{gathered} \tag{1}$$

These relations mean that the projection of the velocity of the center of mass of each wheel pair C_1 and C_2 onto the direction perpendicular to the plane of the corresponding wheel is equal to zero (see also [12]).

Instead of the generalized velocities $\dot{\boldsymbol{q}} = (\dot{x}, \dot{y}, \dot{\psi})$, it is convenient in this case to pass to the quasi-coordinates $\boldsymbol{v} = (v_1, v_2)$ and ω, where $\boldsymbol{v}$ is the velocity of point P referred to the axes of the moving coordinate system $C_1x_1y_1$, and ω is the absolute angular velocity of the first platform:

$$v_1 = \dot{x}\cos\psi + \dot{y}\sin\psi, \quad v_2 = -\dot{x}\sin\psi + \dot{y}\cos\psi, \quad \omega = \dot{\psi}.$$

The constraint equations (1) in the new variables become

$$\begin{gathered} v_2 + c_1\omega = 0, \\ v_1\sin\varphi(t) - v_2\cos\varphi(t) + c_2(\omega + \dot{\varphi}(t)) = 0. \end{gathered} \tag{2}$$

In [5] it is shown that in the case where the angle $\varphi(t)$ between the platforms is a prescribed function of time, the equation governing the evolution of the linear velocity of the first platform v_1 can be written as

$$\dot{v}_1 = \big(A(t) - C(t)\big)v_1 + B_1(t) + B_2(t) - D(t), \tag{3}$$

where

$$\begin{gathered} A(t) = -\frac{\dot{\varphi}\sin\varphi(J_1S_2 + \delta S_1)}{S_1(J_1\sin^2\varphi + MS_1^2)}, \\ B_1(t) = \frac{\ddot{\varphi}\sin\varphi(J_1c_2 - J_2S_1)}{(J_1\sin^2\varphi + MS_1^2)} \\ B_2(t) = \frac{\dot{\varphi}^2(J_1c_1c_2\sin^2\varphi - S_1(c_1\delta\cos\varphi + \varepsilon c_2S_1))}{S_1(J_1\sin^2\varphi + MS_1^2)} \\ C(t) = 2\frac{(b_1^2k_1 + b_2^2k_2)\sin^2\varphi + k_1S_1^2 + k_2S_2^2}{J_1\sin^2\varphi + MS_1^2}, \\ D(t) = 2\frac{\dot{\varphi}\sin\varphi\big(c_1k_2(b_2^2 - c_2^2)\cos\varphi - c_2(b_1^2k_1 + c_1^2k_2)\big)}{J_1\sin^2\varphi + MS_1^2}, \\ S_1 = c_1\cos\varphi + c_2, \quad S_2 = c_1 + c_2\cos\varphi. \end{gathered}$$

Here, to abbreviate the formula, we have introduced the following notation:

$$\begin{gathered} M = m_1 + m_2, \quad \delta = c_1a_2m_2 + c_2a_1m_1, \\ \varepsilon = m_1a_1 + c_1m_2, \quad k_1 = \frac{\kappa_1}{h^2}, \quad k_2 = \frac{\kappa_2}{h^2}, \\ J_1 = I_{10} + I_{20} + m_1a_1^2 + m_2(a_2^2 + c_1^2 - c_2^2), \\ J_2 = I_{20} - m_2(c_2^2 - a_2^2). \end{gathered}$$

The evolution of the configuration variables is governed by the system

$$\begin{gathered} \dot{\psi} = -\frac{v_1\sin\varphi(t) + c_2\dot{\varphi}(t)}{c_1\cos\varphi(t) + c_2}, \\ \dot{x} = v_1\cos\psi - c_1\frac{v_1\sin\varphi(t) + c_2\dot{\varphi}(t)}{c_1\cos\varphi(t) + c_2}\sin\psi, \\ \dot{y} = v_1\sin\psi + c_1\frac{v_1\sin\varphi(t) + c_2\dot{\varphi}(t)}{c_1\cos\varphi(t) + c_2}\cos\psi. \end{gathered} \tag{4}$$

In this paper we consider various periodic control functions $\varphi(t)$ given by the general relation

$$\varphi(t) = \alpha\frac{2\pi}{T}\frac{\prod_{n=1}^{N}(2n+1)}{\prod_{n=1}^{N}2n}\int\cos^{(2N+1)}\left(\frac{2\pi t}{T}\right)dt + \varphi_0, \tag{5}$$

where α, φ_0 are constants. The multipliers in front of the integral in (5) are defined in such a way that the maximal deviation of the function $\varphi(t)$ from φ_0 is equal to α, N is an integer defining the "sharpness" of stroke (the velocity of the change of sign of the function $\varphi(t)$ in the middle of a period), see Fig. 2. The larger N, the closer to the vertical the tangent to the function $\varphi(t)$ when $t = T/2$. The simulations were conducted for the period of the control action $T = 1$,

since the selected elements of the control system and the motor could guarantee the specified function of the control action in experiments.

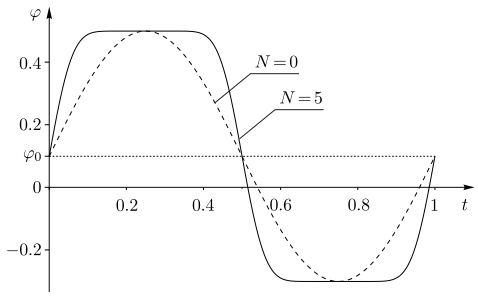

Fig. 2. Graphs of the function $\varphi(t)$ for $N = 0$ and $N = 5$, $\alpha = 0.4, \varphi_0 = 0.1, T = 1$

For $N = 0$ the function $\varphi(t)$ has the simplest form

$$\varphi(t) = \alpha \sin\left(\frac{2\pi t}{T}\right) + \varphi_0. \tag{6}$$

Control of such form was also considered in [5].

In this paper we investigate periodic solutions for different values of α, φ_0, N and define the optimality criteria - the maximum velocity of the Roller Racer for controlled motion (Section III) along a straight line. Section IV presents a comparison between theoretical and experimental results taking the resulting criteria into account.

III. The trajectory of motion in the case of a periodic solution of the reduced system

For brevity, we will write (3) in the form

$$\dot{v}_1 = -\Phi(t)v_1 + \Psi(t), \tag{7}$$

where $\Phi(t)$ and $\Psi(t)$ are functions that are periodic with the same period T in the case of periodic controls $\varphi(t)$ (Eq.(5)).

In [5] it is proved that the following proposition holds.

Proposition 1. *For positive (friction) coefficients $k_1 > 0$ and $k_2 > 0$ Eq. (7) has a partial solution periodic in time, $v_1 = Q(t)$, to which all trajectories of Eq. (7) tend as $t \to +\infty$.*

$$Q(t) = \frac{1}{P(t)(P(T)-1)} \int_0^T \Psi(\tau)P(\tau)d\tau + \frac{1}{P(t)} \int_0^t \Psi(\tau)P(\tau)d\tau, \tag{8}$$

where

$$P(t) = e^{\int_0^t \Phi(\tau)d\tau}. \tag{9}$$

It is easy to show that the function $P(t)$ is not periodic and satisfies the relation

$$P(t+T) = P(T)P(t), \quad P(T) > 1. \tag{10}$$

A. Periodic motion with $\varphi_0 = 0$

.

In this section we show that, in the case of control actions $\varphi(t)$ (Eq.(5)) with $\varphi_0 = 0$, the point of contact of the platforms, P, moves periodically, uniformly shifting, along a straight line or a circle

We first formulate two auxiliary lemmas which are satisfied by $T-$periodic functions.

Lemma 1. If a T-periodic function $F(t)$ is antisymmetric relative to the shift by $\Delta t = T/2$, that is, if it satisfies the relation

$$F(t) = -F(t + T/2), \tag{11}$$

then the value of this function averaged over a period is zero:

$$\langle F \rangle = \frac{1}{T} \int_0^T F(t)dt = 0. \tag{12}$$

Lemma 2. If the right-hand side of the differential equation

$$\dot{f}(t) = F(t) \tag{13}$$

is a T-periodic function and satisfies relation (11), then the function $f(t)$ is $T-$periodic (without a linear increase).

We note that for the chosen controls in the form (5) with $\varphi_0 = 0$ the following relations hold:

$$\varphi(t) = -\varphi(t + T/2), \quad \dot{\varphi}(t) = -\dot{\varphi}(t + T/2). \tag{14}$$

Then it follows from (3), (7) and (14) that the functions $\Psi(t)$ and $Q(t)$ are $T/2$-periodic, i.e., the following relations hold:

$$\Psi(t) = \Psi(t + T/2), \quad Q(t) = Q(t + T/2). \tag{15}$$

In view of Eq. (5) with $v_1 = Q(t)$ it follows from the equation for $\dot{\psi}$ (4) that its right-hand side is a T-periodic function, which we denote by $F(t)$ for brevity:

$$\dot{\psi}(t) = F(t), \quad F(t) = F(t + T). \tag{16}$$

On the other hand, directly substituting (14) and (15) into the function $F(t)$ yields

$$F(t) = -F(t + T/2). \tag{17}$$

In this case, by Lemma 2, *the function $\psi(t)$ is $T-$periodic*. We represent it as a sum of the T-periodic function with zero mean and a constant:

$$\psi(t) = \Psi_0(t) + \psi^*,$$
$$\Psi_0(t) = \Psi_0(t + T), \quad \langle \Psi_0 \rangle = 0, \quad \psi^* = \langle \psi \rangle = \text{const}.$$

Let us rotate the initial coordinate system through angle ψ^*. In the new (rotated) fixed coordinate system the function $\Psi_0(t)$ will define the orientation of the first platform.

With the previous remarks in mind, we integrate the equation for $\dot{\psi}$ (16) and obtain

$$\Psi_0(t) = \int_0^t F(\tau)d\tau - \frac{1}{T} \int_0^T d\tau \int_0^\tau F(z)dz. \tag{18}$$

As noted above, the function $\Psi_0(t)$ has zero mean value. In addition, it can be explicitly shown that for this function a more rigorous statement holds.

Proposition 2. *In the case of periodic controls* (5) *with* $\varphi_0 = 0$ *the function* $\Psi_0(t)$ (18) *is antisymmetric relative to the shift by* $\Delta t = T/2$*, i.e., the following relation holds:*

$$\Psi_0(t) = -\Psi_0(t + T/2). \tag{19}$$

Now, from the equations for $\dot{x}, \dot{y}$ (4) it can be shown by direct substitution that after rotation of the coordinate system through angle ψ^* with $v_1(t) = Q(t)$, taking (14), (15) and (19) into account, the following relations hold:

$$\dot{x}(t) = \dot{x}(t + T/2), \quad \dot{y}(t) = -\dot{y}(t + T/2). \tag{20}$$

Thus, by Lemma 2, with (4) and (20) taken into account, the following proposition holds.

Proposition 3. *In the case of periodic controls* (5) *with* $\varphi_0 = 0$ *the following relations hold for the coordinates* (x, y) *of the point of contact of the platforms, P:*

$$\begin{gathered} x(t) = k_x t + X(t), \quad y(t) = Y(t), \\ X(t) = X(t + T/2), \quad Y(t) = Y(t + T), \end{gathered} \tag{21}$$

$$\begin{aligned} k_x = \frac{2}{T} \int_0^{T/2} \Big(& Q(t) \cos \Psi_0(t) \\ & - c_1 \frac{Q(t) \sin \varphi(t) + c_2 \dot{\varphi}(t)}{c_1 \cos \varphi(t) + c_2} \sin \Psi_0(t) \Big) \, dt, \end{aligned} \tag{22}$$

that is, the point of attachment of the platforms, P, moves periodically, uniformly (with velocity k_x*), shifting along the axis rotated through angle* ψ^* *relative to the axis* Ox *of the initial coordinate system.*

The shift velocity k_x depends on the control parameters α and N. Figure 3 shows graphs of the function $k_x(\alpha)$ for different values of N. The graphs are plotted for the Roller Racer's parameters presented in Table II.

TABLE II
THE ROLLER RACER'S PARAMETERS

platform	m_i, kg	a_i, m	c_i, m	$I_{0i}, kg \cdot m^2$	b_i, m
I	0.61	0.029	0.19	0.034	0.077
II	0.33	0.0013	0.05	0.009	0.075

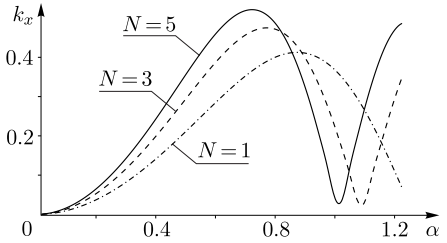

Fig. 3. Graphs of the function $k_x(\alpha)$ for $N = 1, 3, 5$; $\varphi_0 = 0, T = 1$

The dependences thus obtained suggest that

1. *the average shift velocity* k_x *increases as the value of* N *increases*;
2. *there exists an optimal value of the amplitude of the function* $\varphi(t)$ *at which the average shift velocity* k_x *is maximal.*

IV. EXPERIMENT

Using the equipment of the Common Use Center of the Udmurt State University, the Laboratory of Mobile Systems (Kalashnikov Izhevsk State Technical University) has fabricated a prototype of the Roller Racer, for which a 3D Roller Racer model was designed in the software product Solid Works (Fig. 4). Its mass and geometric characteristics are presented in Table II.

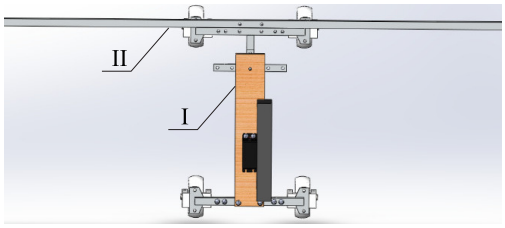

Fig. 4. 3D model of the Roller Racer

The prototype was placed onto a flat even surface. To record the trajectory and the turning angles of the frame, light-reflecting markers for the VICON motion capture system were placed on the large (I) and small (II) platforms.

When conducting the experiments, restrictions on the maximal relative deviation angle of the platforms and the velocities of rotation of the servodrive were taken into account. For this specimen the maximal deviation was $\alpha = 0.8$ rad.

In the course of the experiments, the initial stage where the motion becomes periodic was, as a rule, not taken into account. Therefore, the initial position of the Roller Racer on the experimental trajectory and that on the trajectory obtained by modeling do not exactly coincide in the graphs below.

To smooth the output data from the VICON motion capture system, a running average Matlab function for smoothing the jumps in output data was applied.

The fabricated prototype has some design constraints which influence the experimental data. These include deviation of the value of φ_0 from zero value. The average value of the angle of shift for the developed prototype is 0.01 rad. This is no more than 4 % of the value of the oscillation amplitude of the function, but, as a result, the point P of attachment of the platforms which moves in a generally straight line shifts to either side. In addition, the torque characteristics of the drive do not allow acceleration and deceleration to be ensured when $N > 5$.

To determine the qualitative dependence of the trajectory of point P and the average velocity of motion of the system on two parameters, α and N, we have carried out two series of experiments (5 for each set of parameters):

1. for $N = 5$ with two different amplitudes $\alpha_1 = 0.3$ rad and $\alpha_2 = 0.5$ rad, $T = 1$;

2. for $N = 1$ and $N = 5$ with $\alpha = 0.3 \pm 0.05$, $T = 1$.

The initial conditions for simulations taking into account the initial relative position of the platforms, the orientation of the Roller Racer were determined from experiments.

Figures 5 and 6 show the trajectories of point P with $N = 5$ for two different amplitudes, $\alpha_1 = 0.3$ rad and $\alpha_2 = 0.5$. The corresponding average velocities of motion of point P are $k_{x1} = 0.13$ m/s and $k_{x2} = 0.35$ m/s. Not only a qualitative, but also a quantitative coincidence of the dependence $k_x(\alpha)$ is observed.

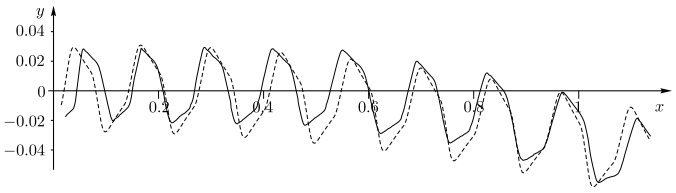

Fig. 5. The experimental (solid line) and theoretical (dashed line) trajectories of the Roller Racer for $N = 5, \alpha_1 = 0.3, T = 1$

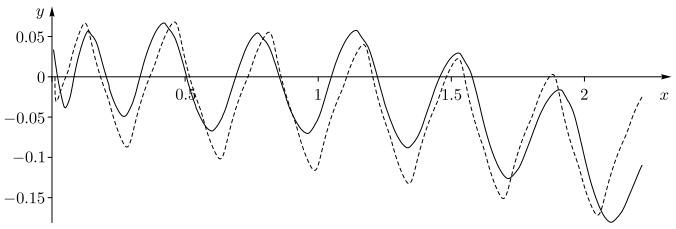

Fig. 6. The experimental (solid line) and theoretical (dashed line) trajectories of the Roller Racer for $N = 5, \alpha_1 = 0.5, T = 1$

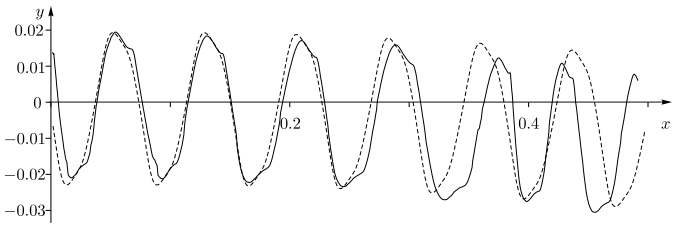

Fig. 7. The experimental (solid line) and theoretical (dashed line) trajectories of the Roller Racer for $N = 1, \alpha_1 = 0.27, T = 1$

Figures 5 and 7 show the trajectories of point P with $N = 1$ for $\alpha_1 = 0.27$ and $N = 5$ for $\alpha_2 = 0.3$. The corresponding average velocities of motion of point P are $k_{x1} = 0.077$ m/s and $k_{x2} = 0.13$. Thus, as the values of N increases, the value of k_x increases. By analogy with the previous comparison, not only a qualitative, but also a quantitative coincidence of the dependence $k_x(\alpha)$ is observed.

The deviations of the experimental trajectories from simulated ones, as in experiments of a similar system [13], stem from errors made in manufacturing and assembling the mobile robot, backlash at the joint and possible slipping of the wheels.

V. Conclusion

In this paper, we have investigated the controlled motion of the Roller Racer on a plane, depending on control parameters. It has been shown that for the chosen control the system moves periodically in a generally straight line. The velocity of this motion increases with increasing amplitude of oscillations of the control function and with increasing parameter N, which defines the velocity of the relative stroke of the second platform in the middle of the period of oscillation of the control function. This dependence has been defined theoretically and confirmed experimentally.

Acknowledgment

The authors express their appreciation to I. S.Mamaev and I. A. Bizyaev for useful discussions of the results obtained.

References

[1] Martynenko Yu. G., "Motion Control of Mobile Wheeled Robots", J. Math. Sci. (N. Y.), 2007, vol. 147, no. 2, pp. 6569–6606.

[2] Bloch A. "Nonholonomic mechanics and control", Springer, 2003, 501 p.

[3] Rocard Y. "L'instabilité en mécanique: Automobiles, avions, ponts suspendus", Paris: Masson, 1954.

[4] Bizyaev I. A. "The Inertial Motion of a Roller Racer", Regular and Chaotic Dynamics, 2017, vol. 22, no. 3, pp. 239–247.

[5] Bizyaev I. A., Borisov A. V., Mamaev I. S., "Exotic Dynamics of Nonholonomic Roller Racer with Periodic Control", Regular and Chaotic Dynamics, 2018, vol. 23, no. 7-8, pp. 983–994

[6] Borisov A. V., Mamaev I. S., Kilin A. A., Bizyaev I. A., " Qualitative Analysis of the Dynamics of a Wheeled Vehicle", Regular and Chaotic Dynamics, 2015, vol. 20, no. 6, pp. 739–751.

[7] Borisov A. V., Kilin A. A., Mamaev I. S., "On the Hadamard–Hamel Problem and the Dynamics of Wheeled Vehicles", Regular and Chaotic Dynamics, 2015, vol. 20, no. 6, pp. 752–766.

[8] Krishnaprasad, P. S., and Dimitris P. Tsakiris."Oscillations, SE (2)-snakes and motion control: A study of the roller racer," Dynamical Systems: An International Journal, 2001, vol. 16, no. 4, pp. 347-397.

[9] Fedonyuk, V., and Tallapragada, P., "Locomotion of a Compliant Mechanism with Nonholonomic Constraints," ASME. J. Mechanisms Robotics, 2020, pp. 1 —13, doi: https://doi.org/10.1115/1.4046510

[10] Bullo, F., and Lewis, A. D., "Kinematic controllability and motion planning for the snakeboard," IEEE Transactions on Automatic Control, 2003, 19, pp. 494 —498.

[11] Shammas, E., de Oliveira, M."Motion planning for the Snakeboard," The International Journal of Robotics Research, 2012, vol. 31, no. 7, 872 — 885. https://doi.org/10.1177/0278364912441954

[12] Bizyaev I. A., Borisov A. V., Mamaev I. S., "Dynamics of the Chaplygin Sleigh on a Cylinder", Regular and Chaotic Dynamics, 2016, vol. 21, no. 1, pp. 136–146.

[13] Ardentov A. A., Karavaev Y. L., Yefremov K. S., " Euler Elasticas for Optimal Control of the Motion of Mobile Wheeled Robots: the Problem of Experimental Realization", Regular and Chaotic Dynamics, 2019, vol. 24, no. 3, pp. 312-328.